Research Article | Vol. 10, No. 10 / 1 October 2020 / Optical Materials Express 2706
Optical Materials EXPRESS

Lightweight metasurface mirror of silicon nanospheres [Invited]

ANDREY B. EVLYUKHIN,[1] MARIIA MATIUSHECHKINA,[2] VLADIMIR A. ZENIN,[3] MICHÈLE HEURS,[2] AND BORIS N. CHICHKOV[1,*]

[1]Institute of Quantum Optics, Leibniz Universität Hannover, Welfengarten 1, 30167 Hannover, Germany
[2]Institut for Gravitational Physics, Leibniz Universität Hannover, Callinstr. 38, 30167 Hannover, Germany
[3]Center for Nano Optics, University of Southern Denmark, Campusvej 55, 5230 Odense, Denmark
*chichkov@iqo.uni-hannover.de

Abstract: Many experiments in modern quantum optics require the implementation of lightweight and near-perfect reflectors for noise reduction and high sensitivity. Another important application of low mass and high reflectivity mirrors is related to the development of solar or laser-driven light sails for acceleration of ultra-light spacecrafts to relativistic velocities. Here, we present numerical results and theoretical analysis of a metasurface mirror consisting of periodically arranged silicon nanospheres embedded in a polymer. In the absence of material losses or disorder, this mirror demonstrates absolute 100% reflection at a single wavelength, which can be tuned by changing nanosphere dimensions or periodicity (for example, by mechanical stretching). We show that high reflectivity can be reached due to electric or magnetic dipole resonant responses of Si nanoparticles in the metasurface. Dependence of mirror reflectivity on surrounding conditions, nanoparticle sizes, and the disorder in the array is studied and discussed. The optimization and simulation procedures presented in this work can be used for the development of other optical devices with functional characteristics determined by the resonant interaction of light with metasurfaces made of nanospheres.

1. Introduction

The growing interest in the ability to create small sensitive detectors of weak mechanical forces and vibrations has stimulated investigations in the fields of optomechanical sensors, cavity optomechanics, and quantum noise reduction devices [1,2]. One of the main optical components in such systems is a low mass and high reflectivity mirror which can be used as a suspended mirror in optical resonators and interferometers. Low mass and high reflectivity mirrors are also required for the realization of solar or laser-driven light sails for acceleration of nano-satellites to relativistic velocities and their exploratory missions to nearby stars and exoplanets [3–5].

For the design and fabrication of such mirrors different optical configurations and materials have been investigated during the last years. One of the approaches in the field of optomechanics is related to the application of artificial metamaterials [6] composed of specially designed building blocks (meta-atoms) determining optical and mechanical properties of the total system and its functional characteristics. In contrast to three-dimensional (3D) metamaterials, which are used for control and manipulation of light in spectral, spatial, and temporal domains, two-dimensional (2D) single layer artificial structures, called metasurfaces, provide unique possibilities for light management and control at the subwavelength scale. In this case, strong light-matter interaction is reached due to resonant optical responses of meta-atoms building the metasurface [7]. For minimisation of light absorption in artificial structures, dielectric high-refractive index nanoparticles are used as building blocks, for example, crystalline silicon nanoparticles with negligibly small absorption in near-infrared. Due to the high refractive index ($n_{\mathrm{Si}} = 3.56$ at $\lambda = 1064$ nm), the sizes of Si nanoparticles supporting the optical resonant response can be n_{Si}-times smaller than the free-space wavelength of light [8]. All these properties

#409311 https://doi.org/10.1364/OME.409311
Journal © 2020 Received 2 Sep 2020; accepted 11 Sep 2020; published 30 Sep 2020

Optical Materials EXPRESS

of silicon nanoparticles make them very promising candidates for the development of ultra-thin metasurfaces with different optical functionalities [9,10].

In this article, we suggest a straightforward design and numerical optimization procedure for a low mass mirror based on the spherical nanoparticle structure that allows to achieve extremely high incident-light reflectivity. This mirror is specially designed for optomechanical applications and the detection of weak physical forces. Note that the same metasurface mirror concept can be used for the realization of light sails. For practical realization of low mass, high reflectivity metasurface mirrors, laser printing of Si nanoparticles is discussed as a promising technology.

The proposed mirror consists of silicon nanoparticles arranged in a 2D subwavelength periodic array embedded in a polymer elastomer layer of polydimethylsiloxane (PDMS). The size of the particles and the distance between them are optimized to achieve maximum reflectivity of the normally incident plane-wave at the near-infrared wavelength of 1064 nm. In this spectral range, silicon and PDMS exhibit negligibly low absorption which allows to use this mirror in experiments where light-induced material heating is undesirable [11,12]. Our metasurface design with only a single layer of nanoparticles allows realization of a thin and lightweight mirror, which is beneficial over multilayer mirrors usually implemented in mechanical resonators [13,14].

The reflection and transmission of the metasurface is analyzed in the framework of excited nanoparticle multipole resonances [15]. It is important to note that the suppression of light transmission is not related to the light absorption, but rather to the destructive interference between incident and resonantly scattered light in the forward direction. Dielectric nanospheres support Mie resonances corresponding to the excitation of their different multipole moments. As will be shown in this article, resonant electric or magnetic dipole scattering can completely cancel the transmission and provide the near-unity reflection for the light at the target wavelength of 1064 nm. How to reach high reflectivity in all-dielectric metamaterial structures has recently been investigated using the effective medium approach (EMA) [16]. In our work we apply a completely different approach, namely direct multipole analysis, which provides an intuitive understanding, a rather good match to the simulations, and simplifies the design optimization for the desired wavelength.

The modelling approach presented in this work is based on full-wave numerical simulations and semi-analytical calculations developed in the framework of the coupled dipole approximation [10]. We show that by tuning the array periodicity, it is always possible to get a near-unity reflectance at a desired light wavelength for any particle diameter within a reasonable range. An estimate of the metasurface mirror robustness to possible imperfections in terms of deviations of nanoparticle sizes and their positions is obtained by numerical simulations. The simulated perfect reflection and suppressed transmission effect by our metasurface mirror agrees well with the coupled dipole model.

In the sections below, basic parameters of the considered mirror system and applied calculation approaches are discussed. Then, the obtained results are demonstrated and analysed. Finally, a short summary of our research is given.

2. Physical model and calculation methods

2.1. Physical system and parameters

Schematic presentation of metasurface considered in this paper is shown in Fig. 1. A periodic 2D array of spherical silicon nanoparticles is placed in a surrounding dielectric matrix with the refractive index n_{d}. The light beam, considered as a monochromatic plane wave with linear polarization, is normally incident along the z-axis of the Cartesian coordinate system illuminating all nanoparticles in the metasurface. The electric field of the incident wave is $\mathbf{E} = (E_x, 0, 0)\exp(ik_{\mathrm{d}}z - i\omega t)$, where k_{d} is the wave number in the surrounding matrix, ω is the angular frequency. In the following, the time dependence $\exp(-i\omega t)$ will be omitted. In our investigations we consider three different surrounding conditions: i) the array is placed in an

Optical Materials EXPRESS

infinite surrounding PDMS matrix with $n_{\mathrm{d}} = 1.45$; ii) the surrounding PDMS matrix occupies only semi-infinite space with the other half-space being air; iii) the nanoparticle array is placed inside a finite size PDMS membrane suspended in air. The refractive index of silicon in the considered near-infrared region (around the target wavelength of 1064 nm) is assumed to be constant $n_{\mathrm{Si}} = 3.56$ without any absorption losses [17]. All wavelengths correspond to free space.

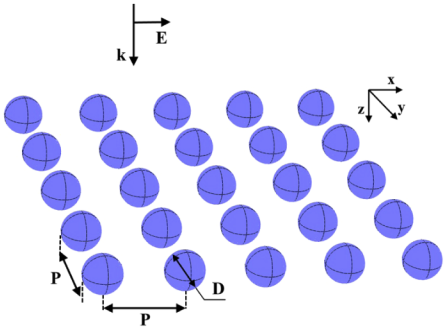

Fig. 1. Schematic view of the considered metasurface, composed of nanospheres, arranged in a square lattice, and definition of basic parameters. The metasurface is irradiated by a plane monochromatic light wave at normal incidence.

2.2. Calculation approaches

In our numerical simulations, the total electric fields and corresponding reflection and transmission spectra in the considered system with spherical nanoparticles, building an infinite-size metasurface, and embedded in a PDMS matrix, are calculated using the finite element method, implemented in the commercial software COMSOL Multiphysics.

For analytical calculations, the coupled dipole approximation (CDA) with the inclusion of only electric and magnetic dipoles is used. Details of this approach are presented elsewhere [10]. Briefly, every particle in the array is considered as a combination of point electric and magnetic dipoles, located at the particle's center. The electric $\mathbf{p}_j$ and magnetic $\mathbf{m}_j$ dipole moments of the j-th particle in the array are determined by the following equations

$$\mathbf{p}_j = \alpha_p \mathbf{E}_{\mathrm{loc}}\,, \qquad \mathbf{m}_j = \alpha_m \mathbf{H}_{\mathrm{loc}} \tag{1}$$

where $\mathbf{E}_{\mathrm{loc}}$ and $\mathbf{H}_{\mathrm{loc}}$ are the local electric and magnetic fields, respectively, acting on the particle, including fields of the incident external wave and fields generated by all other particles in the array. The dipole polarizabilities α_p and α_m of a spherical particle can be found from Mie theory [18]. In our case we can write [10]

$$\alpha_p = i\frac{6\pi\varepsilon_0\varepsilon_{\mathrm{d}}}{k_{\mathrm{d}}^3}a_1, \quad \alpha_m = i\frac{6\pi}{k_{\mathrm{d}}^3}b_1,$$

where i is the imaginary unit, ε_0 and $\varepsilon_{\mathrm{d}} = n_{\mathrm{d}}^2$ are the vacuum dielectric constant and the relative dielectric constant of the surrounding matrix, a_1 and b_1 are the corresponding scattering coefficients [18].

Due to the periodicity of the geometry and the external field, all particles in the array have the same electric and magnetic dipole moments. In this case the field reflection r and transmission t coefficients are determined only by the elementary cell area $S_L = P^2$ containing one particle, the incident light wavelength, and the effective electric α_p^{eff} and magnetic α_m^{eff} dipole polarizabilities

Optical Materials EXPRESS

[10]:

$$r = \frac{ik_{\mathrm{d}}}{2S_L}\left[\alpha_p^{\mathrm{eff}} - \alpha_m^{\mathrm{eff}}\right], \tag{2}$$

$$t = 1 + \frac{ik_{\mathrm{d}}}{2S_L}\left[\alpha_p^{\mathrm{eff}} + \alpha_m^{\mathrm{eff}}\right]. \tag{3}$$

The above equations are applicable when the array periods are smaller than the light wavelength in the surrounding matrix and, therefore, light diffraction is absent [10]. It should be noted that when the particle size becomes large, such that higher-order multipole moments are no longer negligible, or when higher accuracy is required, one should include higher-order terms into the above equations [19]. The effective particle polarizabilities are determined by the single particle dipole polarizabilities and interparticle electromagnetic interactions:

$$\alpha_p^{\mathrm{eff}} = \left(\frac{\varepsilon_0\varepsilon_{\mathrm{d}}}{\alpha_p} - S_p\right)^{-1}, \qquad \alpha_m^{\mathrm{eff}} = \left(\frac{1}{\alpha_m} - S_m\right)^{-1}, \tag{4}$$

where S_p and S_m are the lattice dipole sums for electric-electric dipole and magnetic-magnetic dipole interactions, respectively. For arrays with a square elementary cell, $S_m = S_p$ (analytical expressions for S_p and S_m can be found, for example, in [19]).

The intensity reflection R and transmission T coefficients are determined as

$$R = |r|^2, \qquad T = |t|^2. \tag{5}$$

As follows from Eqs. (3) and (5), the necessary (but not sufficient) condition for $T \to 0$ is given by

$$\mathrm{Re}(\alpha_p^{\mathrm{eff}}) = -\mathrm{Re}(\alpha_m^{\mathrm{eff}}). \tag{6}$$

When $\alpha_p^{\mathrm{eff}} = \alpha_m^{\mathrm{eff}}$, the lattice Kerker effect is realized [10,20] and, as follows from Eq. (2), the reflection is absent.

3. Results and discussion

3.1. Basic configurations

The final goal of our investigations is the realization of a metasurface mirror with strong reflection at a certain incident wavelength $\lambda = 1064$ nm (in vacuum), chosen due to the availability of powerful and ultra-stable lasers at this wavelength. Using facilities of COMSOL Multiphysics, the intensity reflection and transmission coefficients for infinite Si-nanoparticle arrays embedded in surrounding PDMS ($n_{\mathrm{d}} = 1.45$) are calculated as a function of the particle diameter D and the array period P (the array geometry is shown in Fig. 1). Results of the full-wave simulations are demonstrated in Fig. 2.

In Fig. 2(a) one can see that the reflection coefficient R can approach unity for almost any particle diameter D, when the array period P is optimum. Since there are no absorption losses in the system, meaning $R + T = 1$, the proximity of R to 1 can be derived from the proximity of T to 0. Moreover, the absence of losses allows reaching absolute 0 and 1 for R and T at the desired wavelength (Fig. 2).

Even though the system is quite simple (dielectric spheres, arranged in a square lattice), it allows different operation regimes, among which we highlighted two [see circles in Fig. 2(a,b) and corresponding spectra in Fig. 2(c)]. When the particle diameter is $D = 248$ nm and periodicity $P = 719$ nm (point #1), there is a close spectral proximity between suppressed reflection and suppressed transmission. Therefore, one can exploit such a configuration for modulation applications, for example, by stretching the array, heating it, or changing the incident wavelength. Another interesting point (point #2) is selected where the change of the sphere diameter does not

Optical Materials EXPRESS

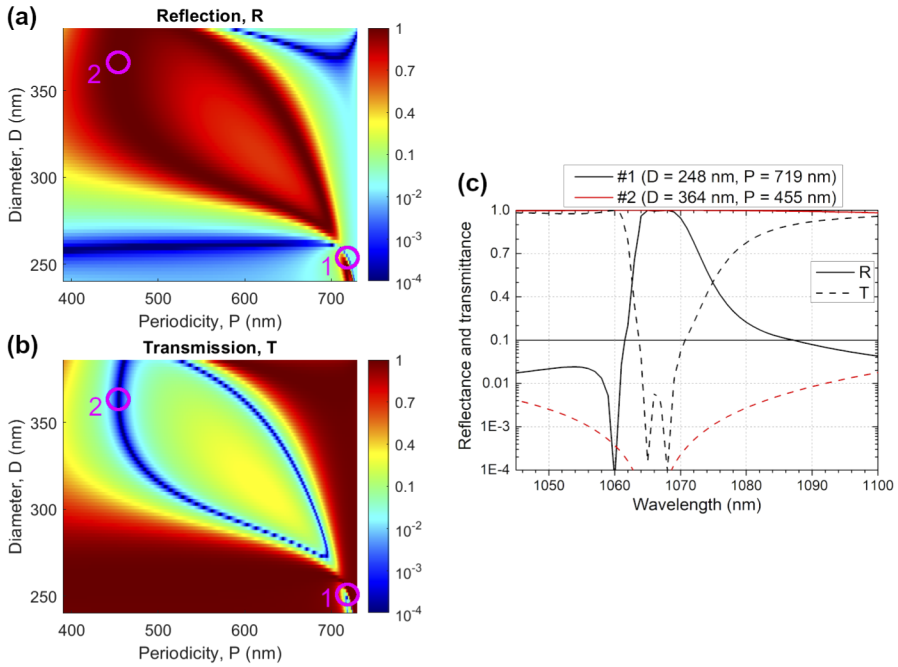

Fig. 2. (a) Reflection and (b) transmission coefficients of metasurfaces calculated as a function of the particle diameter and the array period. The surrounding matrix is PDMS with the refractive index 1.45. Irradiation conditions are the same as shown in Fig. 1, with the free-space wavelength of 1064 nm. Note hybrid colormap scale, used to enhance the perception of values near zero and 1. (c) Reflection and transmission spectra of metasurfaces for two selected sets of parameters (P and D), particularly promising for modulation (black, point #1), broadband reflector (red, point #2).

influence the reflection and transmission. It appeared that for this configuration our metasurface behaves as a broadband near-perfect reflector.

Even though broadband operation (point #2) could be advantageous for our goal, the realistic fabrication of such structures might be extremely difficult due to the proximity of particle diameter to the periodicity. Therefore, we have chosen realistic configurations with a particle diameter of $D = 290$ nm and two array periodicities: $P = 602$ nm and $P = 686$ nm, both featuring complete reflection at the free-space wavelength of 1064 nm (Fig. 3).

In order to clarify physical mechanisms responsible for such high reflection, we apply the CDA described above. The silicon nanoparticles in metasurface arrays are considered as point electric and magnetic dipoles with moments defined by the corresponding polarizabilities. In Fig. 3, the reflection and transmission spectra calculated by analytical and numerical methods are presented. One can see that the CDA provides reasonably good agreement in the reflection and transmission spectra with the numerical simulations. In both cases, high reflection is reached at the same wavelength of 1064 nm. In the CDA the reflection and transmission coefficients [Eqs. (2) and (3)] are determined by the effective polarizabilities [Eq. (4)]. Their spectral behaviour is shown in Fig. 4. For the period $P = 602$ nm [see Fig. 4(a)], the magnetic dipole effective polarizability α_m^{eff} has a broad resonance at the wavelength $\lambda \approx 1075$ nm. As a result, α_m^{eff} gives the main contribution into the coefficients r and t and is responsible for the transmission suppression. The non-resonant contribution of α_p^{eff} only provides an additional small spectral tuning of the reflection maximum to $\lambda \approx 1064$ nm, owing to the necessary condition of Eq. (6). For better visualization, the $\text{Re}(\alpha_m^{\text{eff}})$ is plotted with a negative sign, and the crossing with $\text{Re}(\alpha_e^{\text{eff}})$, highlighted with a

Optical Materials EXPRESS

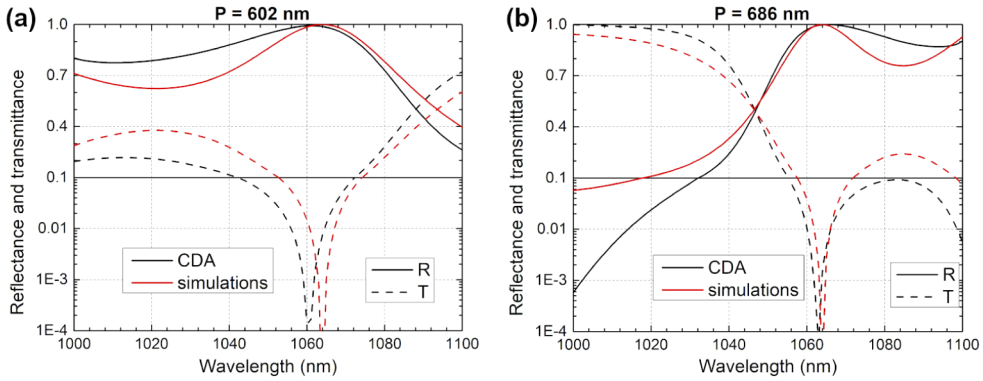

Fig. 3. Comparison between the coupled dipole approximation (CDA) and full-wave numerical simulations, applied to calculate the reflection and transmission spectra for the metasurface with diameter of silicon nanospheres D = 290 nm and periodicity (a) P = 602 nm and (b) P = 686 nm. Irradiation conditions are shown in Fig. 1.

green circle in Fig. 4(a), indicates where this condition is satisfied. It should be noted that the condition of Eq. (6) is also satisfied in another point (at $\lambda \approx 1025$ nm), but there is no total suppression of the transmission at this point, because, as mentioned before, the condition of Eq. (6) is not sufficient.

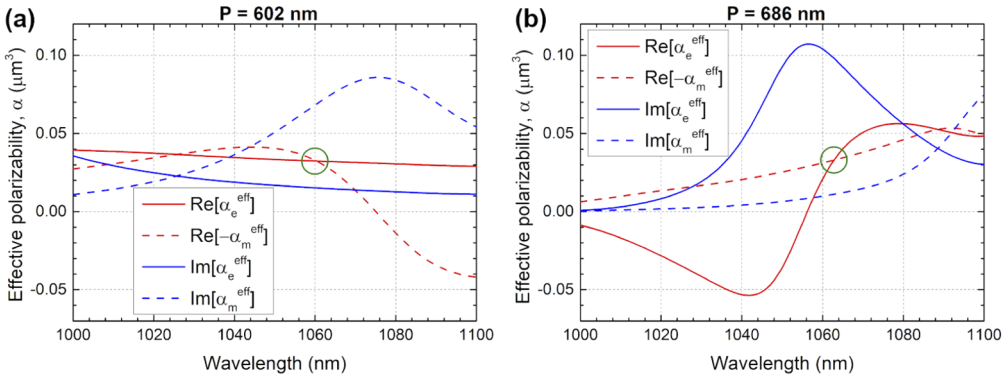

Fig. 4. Effective electric and magnetic dipole polarizabilities, calculated using the coupled dipole approximation for the metasurface arrays with the periods (a) P = 602 nm and (b) P = 686 nm, assuming the nanoparticle diameter D = 290 nm. Green circles indicate the points, where the condition for the complete suppression of transmission [Eq. (6)] is fulfilled.

For the larger period P = 686 nm [see Fig. 4(b)], the electric dipole effective polarizability α_p^{eff} has a resonance at $\lambda \approx 1055$ nm and provides the main contribution into the reflection, whereas the non-resonant contribution of α_m^{eff} slightly corrects the spectral position of the reflection maximum according to the condition of Eq. (6). The green circle in Fig. 3(b) indicates where $\text{Re}(\alpha_p^{\text{eff}}) = -\text{Re}(\alpha_m^{\text{eff}})$. Thus, both magnetic and electric dipole moments, being resonantly excited, can be responsible for the total suppression of the transmission through the metasurfaces. Moreover, each region with the suppressed transmission in Fig. 2(b) can be associated to either electric or magnetic dipole near-resonant excitation. When these two curves are expected to cross (at $D \approx 260$ nm and $P \approx 710$ nm), the perfect reflection is lost and replaced with the perfect transmission. Explanation of this reflection suppression follows from the lattice Kerker effect [10,20]: when the effective electric and magnetic dipole polarizabilities of nanoparticles are

Optical Materials EXPRESS

equal to each other, the reflection is significantly suppressed, because every nanoparticle in the array does not scatter the incident wave into the backward direction [21]. Directly it can be seen from Eq. (2): when $\alpha_p^{\text{eff}} = \alpha_m^{\text{eff}}$, the reflection coefficient $r = 0$. Note that, despite transparency of the metasurface, the polarizabilities of each particle is not zero in this case, but rather resonant, which could be beneficial for non-invasive sensing or non-linear optical applications.

So far we considered that the metasurfaces are embedded in an infinite homogeneous medium (PDMS) with the refractive index of 1.45. However, the near-unity reflection can be also realized when the PDMS surrounding is limited from one or both sides (Fig. 5). Similar to a homogeneous environment (Fig. 2), strong reflection is realized for certain values of the nanoparticle diameter and the array period. Due to the high refractive index contrast of particles relative to the PDMS and air, the partial substitution of PDMS with air does not significantly influence the reflection and transmission, which can be compensated by slightly changing the periodicity of the array in order to reach perfect reflection at 1064 nm. Thus, our perfect metasurface mirror can be extremely lightweight, when Si nanospheres are embedded in thin PDMS membrane [Fig. 5(b)]. When the mirror of the same weight is realized as a silver mirror, its thickness is as low as 30 nm. Since this is close to the skin depth of silver (which is ≈ 24 nm at the wavelength of 1064 nm), the expected reflectivity of such mirror is only ~ 95%.

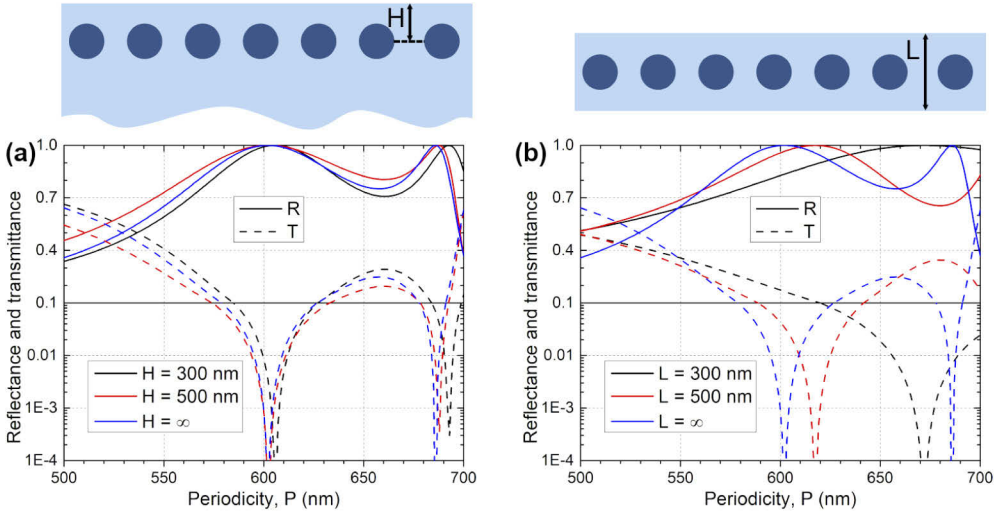

Fig. 5. Reflection and transmission coefficients of metasurface arrays, embedded in PDMS (a) semi-infinite space at different depths H and (b) membrane of finite thickness T (see inserts) as a function of periodicity. All nanoparticles have the same diameter of 290 nm. Irradiation conditions are shown in Fig. 1 and the vacuum wavelength of incident light is 1064 nm.

3.2. *Influence of imperfections*

In real experimental situations arrays of nanoparticles include some structural imperfections related to deviations of the particle sizes and their positions from certain average values. In order to investigate the sensitivity of the reflection coefficient to this type of imperfections we simulate reflection from the infinite metasurface arrays with an elementary cell containing four nanoparicles (Fig. 6). The sizes of the nanoparticles can randomly deviate from the average diameter $D = 290$ nm [Fig. 6(a)]. Additionally, the positions of the nanoparticles in the cell can also randomly deviate from the positions corresponding to perfect periodicity in an ideal array [Fig. 6(b)].

Optical Materials EXPRESS

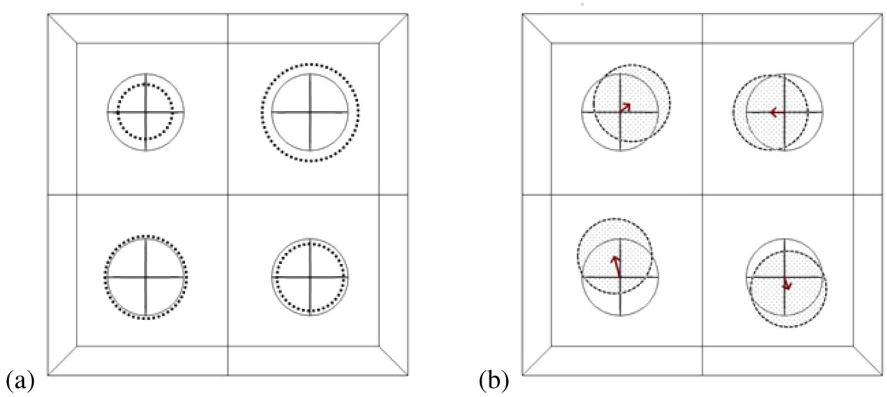

Fig. 6. Schematic presentation of the considered metasurface imperfections. Single elementary cell of periodic arrays with deviations of (a) particle sizes and (b) particle positions from perfect values.

To estimate the decrease in reflectivity, the metasurface structure with an elementary cell consisting of 4 nanoparticles was modelled and simulated using the software COMSOL Multiphysics in combination with Java code. The implementation of two programs allowed to generate random geometry and accumulate the required statistics. Our simulations show that for the maximal random deviation ΔD = 5 nm from the diameter D = 290 nm the average value of the reflection coefficient R is equal to 0.9831 which corresponds to a 1.7% deviation from the ideal case. The random position deviations lead to a reduction of the reflection coefficient which is strongly dependent on the value of the maximum deviation. If the maximum position deviation is 20 nm (3.3% of the period of the ideal array) the reflection coefficient is reduced by 1.5% from the ideal

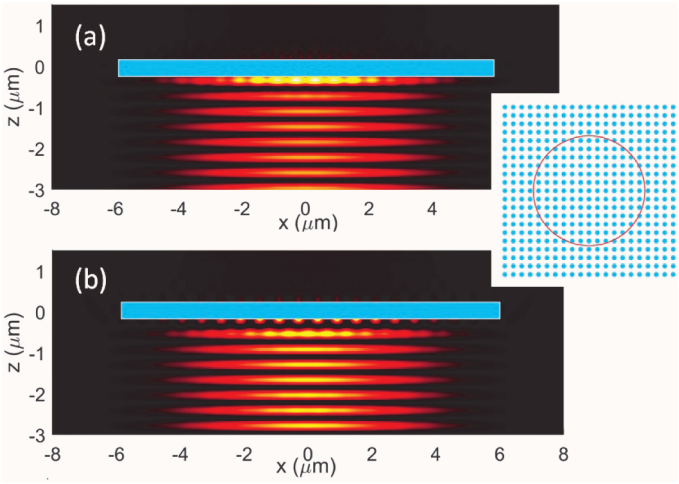

Fig. 7. Strong reflection effect for a Gaussian beam impinging on the finite-size Si nanoparticle metasurface. (a) Intensity of the total electric and (b) magnetic fields calculated in the framework of the CDA [10]. The Gaussian beam (radius of waist is 5 μm) propagates along the z-axis with E-polarization along the x-axis. Position of the metasurface is schematically shown by the blue blocks in (a) and (b). Insert picture demonstrates the nanoparticle structure, and the region inside the red circle is irradiated by the light beam. Parameters: λ = 1064 nm; n_{d} = 1.45; P = 600 nm; D = 290 nm.

Optical Materials EXPRESS

case. However, increasing the maximum deviation up to 6.7% from the period of the ideal array, the reflection coefficient decreases by 18%.

The obtained results and additional simulations carried out in the CDA for a finite-size metasurface structure are shown in Fig. 7. They demonstrate good practical potential of the silicon nanoparticle arrays for the development of ultra-thin and ultra-low mass optical mirrors for optomechanical applications.

4. Practical realization

For practical realization of metasurface mirrors made of Si nanospheres, we plan to apply laser printing technology [22] schematically illustrated in Fig. 8. By illumination of a 50 nm crystalline Si donor layer coated on a glass substrate with a single tightly-focused Gaussian femtosecond laser pulse, absorption in the Si layer leads to ultrafast heating and local melting of this layer. At sufficiently high laser pulse energies, the 50 nm Si layer melts completely, forming a nanodroplet, induced by the surface tension. This nanodroplet formation is accompanied by the motion of its centre-of-mass, driving this droplet towards the PDMS layer on the receiver substrate. During the flight and later contact with the receiver substrate, the nanodroplet will be cooled down and crystallized in the form of spherical nanoparticles. One can vary the nanoparticle diameter by simply changing the laser pulse energy [22]. Due to our preliminary experiments we know that laser printed nanoparticles will be embedded in the PDMS layer. The described process will be performed in air at atmospheric pressure and the distance between the receiver and donor substrates will be set at approximately 10 micrometers. After all nanoparticles are printed, the PDMS layer with the laser printed nanoparticles will be detached from the glass substrate, producing the desired stretchable membrane, acting as a low mass and high reflectivity metasurface mirror.

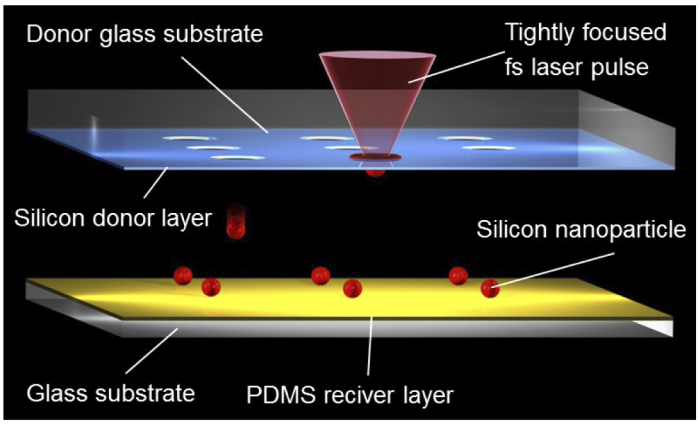

Fig. 8. Schematic illustration of femtosecond laser printing of Si nanoparticles. A 50 nm crystalline Si layer on donor glass substrate wafer is used as a target (irradiated by single laser pulses) to generate and transfer spherical Si nanoparticles onto the PDMS layer.

For fabrication of large mirror arrays, the Si donor layer can be lithographically pre-patterned in the form of periodic circular islands at the required distance between them. In this case many such islands can be melted and transferred by a single laser pulse. This technique has been tested and described in our previous publications [23,24].

Optical Materials EXPRESS

5. Conclusion

In this paper, numerical and analytical calculation methods have been applied for investigations of reflection properties of 2D metasurface arrays, composed of spherical silicon nanoparticles, arranged in a square lattice. Using numerical simulations we have found certain particle sizes and array periods, for which a near-unity reflectivity is achieved for the target near-infrared light wavelength of 1064 nm. It has been shown that the optical response of our metasurface mirror is only weakly influenced by the surrounding conditions, and this influence can be compensated by small adjustments of the periodicity in order to reach perfect reflection at the target wavelength. This allows for realization of perfect and extremely lightweight metasurface mirrors in the form of Si nanoparticles embedded into a polymer membrane. The optical response of the metasurface is explained with analytical coupled dipole approximation, whose results agree well with numerical simulations. Finally, we complited our study by checking the robustness of the real metasurface to possible disorder in terms of random variation in particle size and position.

These mirrors can also be applied as solar or laser-driven light sails for acceleration of ultra-light space craft to relativistic velocities. Practical realization of such metasurface mirrors by laser printing of Si nanoparticles [22] has been discussed.

Funding

Villum Fonden (16498); Deutsche Forschungsgemeinschaft (EXC 2122, Project ID 390833453, EXC 2123, Project ID 390837967).

Acknowledgments

The authors acknowledge financial support from the Deutsche Forschungsgemeinschaft (DFG, German Research Foundation) under Germany's Excellence Strategy within the Cluster of Excellence PhoenixD (EXC 2122, Project ID 390833453) and the Cluster of Excellence QuantumFrontiers (EXC 2123, Project ID 390837967). V.A.Z. acknowledges financial support from Villum Fonden (Grant No. 16498). The analytical analysis has been supported by the Russian Science Foundation Grant No. 20-12-00343.

Disclosures

The authors declare that there are no conflicts of interest related to this article.

References

1. M. Aspelmeyer, T. J. Kippenberg, and F. Marquardt, "Cavity Optomechanics," Rev. Mod. Phys. **86**(4), 1391–1452 (2014).
2. J. Rui, D. Wei, A. Rubio-Abadal, S. Hollerith, J. Zeiher, D. M. Stamper-Kurn, C. Gross, and I. Bloch, "A subradiant optical mirror formed by a single structured atomic layer," Nature **583**(7816), 369–374 (2020).
3. H. A. Atwater, A. R. Davoyan, O. Ilic, D. Jariwala, M. C. Sherrott, C. M. Went, W. S. Whitney, and J. Wong, "Materials challenges for the Starshot lightsail," Nat. Mater. **17**(10), 861–867 (2018).
4. O. Ilic and H. A. Atwater, "Self-stabilizing photonic levitation and propulsion of nanostructured macroscopic objects," Nat. Photonics **13**(4), 289–295 (2019).
5. M. M. Salary and H. Mosallaei, "Photonic metasurfaces as relativistic light sails for Doppler-broadened stable beam-riding and radiative cooling," Laser Photonics Rev. **14**(8), 1900311 (2020).
6. M. A. Noginov and V. A. Podolskiy, *Tutorials in Metamaterials* (CRC Press, 2011).
7. A. E. Minovich, A. E. Miroshnichenko, A. Y. Bykov, T. V. Murzina, D. N. Neshev, and Y. S. Kivshar, "Functional and nonlinear optical metasurfaces," Laser Photonics Rev. **9**(2), 195–213 (2015).
8. A. B. Evlyukhin, S. M. Novikov, U. Zywietz, R. L. Eriksen, C. Reinhardt, S. I. Bozhevolnyi, and B. N. Chichkov, "Demonstration of magnetic dipole resonances of dielectric nanospheres in the visible region," Nano Lett. **12**(7), 3749–3755 (2012).
9. I. Staude and J. Schilling, "Metamaterial-inspired silicon nanophotonics," Nat. Photonics **11**(5), 274–284 (2017).
10. A. B. Evlyukhin, C. Reinhardt, A. Seidel, B. S. Luk'yanchuk, and B. N. Chichkov, "Optical response features of Si-nanoparticle arrays," Phys. Rev. B **82**(4), 045404 (2010).

Optical Materials EXPRESS

11. S. Mancini, V. I. Man'ko, and P. Tombesi, "Ponderomotive control of quantum macroscopic coherence," Phys. Rev. A **55**(4), 3042–3050 (1997).
12. J. D. Thompson, B. M. Zwickl, A. M. Jayich, F. Marquardt, S. M. Girvin, and J. G. E. Harris, "Strong dispersive coupling of a high-finesse cavity to a micromechanical membrane," Nature **452**(7183), 72–75 (2008).
13. J. Steinlechner, I. W. Martin, A. S. Bell, J. Hough, M. Fletcher, P. G. Murray, R. Robie, S. Rowan, and R. Schnabel, "Silicon-based optical mirror coatings for ultrahigh precision metrology and sensing," Phys. Rev. Lett. **120**(26), 263602 (2018).
14. S. Reid and I. W. Martin, "Development of mirror coatings for Gravitational wave detectors," Coatings **6**(4), 61 (2016).
15. V. E. Babicheva and A. B. Evlyukhin, "Resonant suppression of light transmission in high-refractive-index nanoparticle metasurfaces," Opt. Lett. **43**(21), 5186–5189 (2018).
16. B. Slovick, Z. G. Yu, M. Berding, and S. Krishnamurthy, "Perfect dielectric-metamaterial reflector," Phys. Rev. B **88**(16), 165116 (2013).
17. E. Palik, *Handbook of Optical Constant of Solids* (Academic, 1985).
18. C. F. Bohren and D. R. Huffman, *Absorption and Scattering of Light by Small Particles* (Wiley, 1983).
19. V. E. Babicheva and A. B. Evlyukhin, "Analytical model of resonant electromagnetic dipole-quadrupole coupling in nanoparticle arrays," Phys. Rev. B **99**(19), 195444 (2019).
20. V. E. Babicheva and A. B. Evlyukhin, "Resonant lattice Kerker effect in metasurfaces with electric and magnetic optical responses," Laser Photonics Rev. **11**(6), 1700132 (2017).
21. M. Kerker, D. Wang, and C. Giles, "Electromagnetic scattering by magnetic spheres," J. Opt. Soc. Am. **73**(6), 765–767 (1983).
22. U. Zywietz, A. B. Evlyukhin, C. Reinhardt, and B. N. Chichkov, "Laser printing of silicon nanoparticles with resonant optical electric and magnetic responses," Nat. Commun. **5**(1), 3402 (2014).
23. A. I. Kuznetsov, A. B. Evlyukhin, M. R. Gonçalves, C. Reinhardt, A. Koroleva, M. L. Arnedillo, R. Kiyan, O. Marti, and B. N. Chichkov, "Laser fabrication of large-scale nanoparticle arrays for sensing applications," ACS Nano **5**(6), 4843–4849 (2011).
24. A. I. Aristov, U. Zywietz, A. B. Evlyukhin, C. Reinhardt, B. N. Chichkov, and A. V. Kabashin, "Laser-ablative engineering of phase singularities in plasmonic metamaterial arrays for biosensing applications," Appl. Phys. Lett. **104**(7), 071101 (2014).